

Supporting information

Near-infrared Julolidine Probe for Visualization of Mitochondrial Peroxynitrite in Living Cells

Kuppan Magesh¹, Shu Pao Wu², Sivan Velmathi^{1*}

¹Organic and Polymer Synthesis Laboratory, Department of Chemistry, “National Institute of Technology, Tiruchirappalli” – 620 015, India.

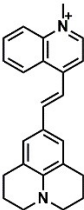
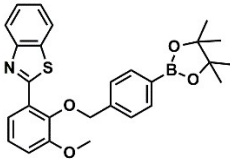
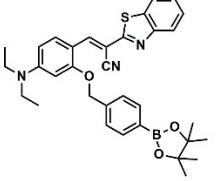
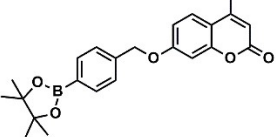
²Department of Applied Chemistry, “National Yang Ming Chiao Tung University, Hsinchu” 30010, “Taiwan, China”

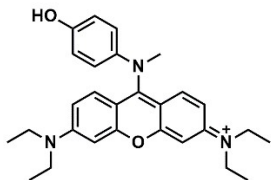
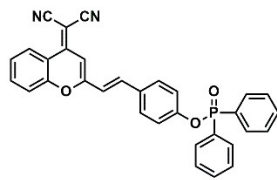
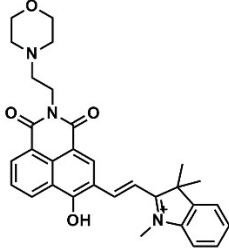
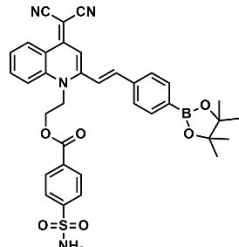
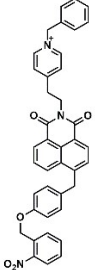
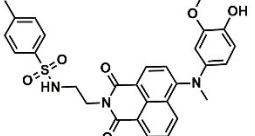
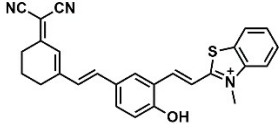
Email: velmathis@nitt.edu

S.NO	Contents	Page No
1	Table S1. A comparative analysis of the proposed probe and the ONOO ⁻ responsive fluorescent probes that are recently reported.	S2-S3
2	Figure S1. ¹ H NMR spectrum of 4-QMe	S4
3	Figure S2. ¹³ C NMR spectrum of 4-QMe	S4
4	Figure S3. ¹ H NMR spectrum of J-CHO	S5
5	Figure S4. ¹³ C NMR spectrum of J-CHO	S5
6	Figure S5. ¹ H NMR spectrum of JQMe	S6
7	Figure S6. ¹³ C NMR spectrum of JQMe	S6
8	Figure S7. HR-ESI Mass spectrum of JQMe	S7
9	Figure S8. ¹ H NMR spectrum of CN-Me	S7
10	Figure S9. ¹³ C NMR spectrum of CN-Me	S8
11	Figure S10. ¹ H NMR spectrum of JCN	S8
12	Figure S11. ¹³ C NMR spectrum of JCN	S9
13	Figure S12. HR-ESI Mass spectrum of JCN	S9
14	Figure S13. (a) The fluorescence spectra of JCN (5 μM) were recorded upon the addition of ONOO ⁻ (10 μM) at various concentrations ranging from 0 to 10 μM. (b) A linear fit was used to plot the JCN emission (5 μM) at 669 nm against the ONOO ⁻ concentration (4–8 μM) (c) The intensity at 669 nm was measured for a probe solution (5 μM) that was mixed with ONOO ⁻ (10 μM) and other analytes in THF-PBS buffer (1:1) (d) The fluorescence intensity of the probe at 669 nm in THF- PBS (1:1) buffer at varying pH levels when combined with ONOO ⁻ (10 μM)	S10
15	Figure S14. Colour change of the probe (20 μM) with different analytes (20 μM) in PBS solution (pH 7.4) under Day light [Analytes: (1) Probe, (2) Al ³⁺ , (3) Ca ²⁺ , (4) Cu ²⁺ , (5) Fe ³⁺ , (6) Mg ²⁺ , (7) Zn ²⁺ , (8) F ⁻ , (9) Cl ⁻ , (10) Br ⁻ (11) I ⁻ , (12) ClO ₄ ⁻ , (13) CN ⁻ , (14) SO ₄ ²⁻ , (15) S ₂ O ₃ ²⁻ , (16) S ₂ O ₄ ²⁻ (17) HS ⁻ , (18) H ₂ O ₂ , (19) HOCl, (20) TBHP, (21) ¹ O ₂ , (22) O ₂ ⁻ , (23) Cys, (24) MesH, (25) Hcy, (26) GSH (27) ONOO ⁻ ,]	S10
16.	Figure S15. (a) The UV-visible absorption spectrum and (b) fluorescence spectra were measured after adding ONOO ⁻ (20 μM) to a JQMe (20 μM) & JCHO (20 μM) in PBS buffer solution (10 mM, 1:1 v/v) at 37 °C	S11

17.	Figure S16. ¹ H NMR titration of JQMe with addition of ONOO ⁻ (0-1.0 eq.)	S11
18.	Figure S17. HR-Mass spectrum of JQMe + ONOO ⁻	S12
19.	Figure S18. Frontier molecular orbital profiles of JQMe (left) and JCHO (right) based on DFT (B3LYP/631 G*)	S12
20.	Figure S19. HOMO and LUMO Hartree value of (a) JQMe and (b) JCHO. The oscillator strength values of (c) JQMe and (d) JCHO.	S13
21.	Figure S20. Cell viability of HeLa cells treated with JQMe (0, 20, 40, 60, 80, 100 μM) at 37°C for 24 h. The results are the mean and standard deviation of three independent experiments.	S13
22.	Table S2. Standard deviation of JQMe (20 μM) without addition of ONOO ⁻ (Ib is the fluorescence intensity at 706 nm)	S14
23.	ESI 1. Limit of detection, limit of quantification, and quantum yield calculation	S14
24.	Table S3. Quantum yield, molar absorptivity and Stokes shift data for JCN and JQMe in different solvents	S14
25.	Table S4. Quantum yield data	S15

Table S1. A comparative analysis of the proposed probe and the ONOO⁻ responsive fluorescent probes that are recently reported.

Probe	λ_{ex} / λ_{em} (nm)	Solvent medium	NIR emission	Detection Limit	Subcellular organelle targeting	Reference
	600/706	PBS buffer	YES	6.5 nM	Mitochondria	This work
	317/483	40% ethanol-PBS buffer	NO	26.3 mmol/L	No	¹
	460/530	10% DMSO-PBS buffer	NO	15 nmol/L	No	²
	322/450	HEPES buffer	NO	29.8 nmol/L	No	³

	440/545	PBS buffer	NO	4 nmol/L	Mitochondria	4
	556/690	50% DMSO-PBS buffer	YES	4.62 μmol/L	No	5
	440/510	50 % Ethanol-PBS buffer	NO	0.24 μmol/L	lysosome	6
	420/600	HEPES buffer	NO	250 nmol/L	Golgi apparatus	7
	453/553	PBS buffer	NO	48 nmol/L	Mitochondrial	8
	488/540	PBS buffer	NO	8.3 nmol/L	Endoplasmic reticulum	9
	500/670	50% MeOH-(Tris-HCl)	YES	10 nmol/L	Mitochondrial	10

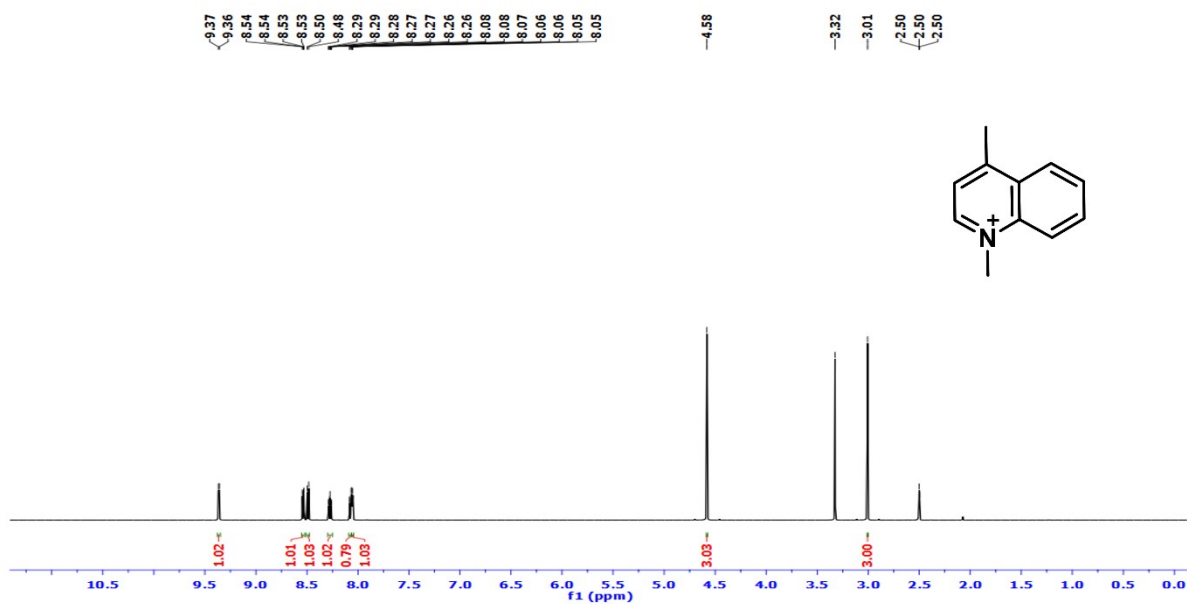


Figure S1. ^1H NMR spectrum of 4-QMe

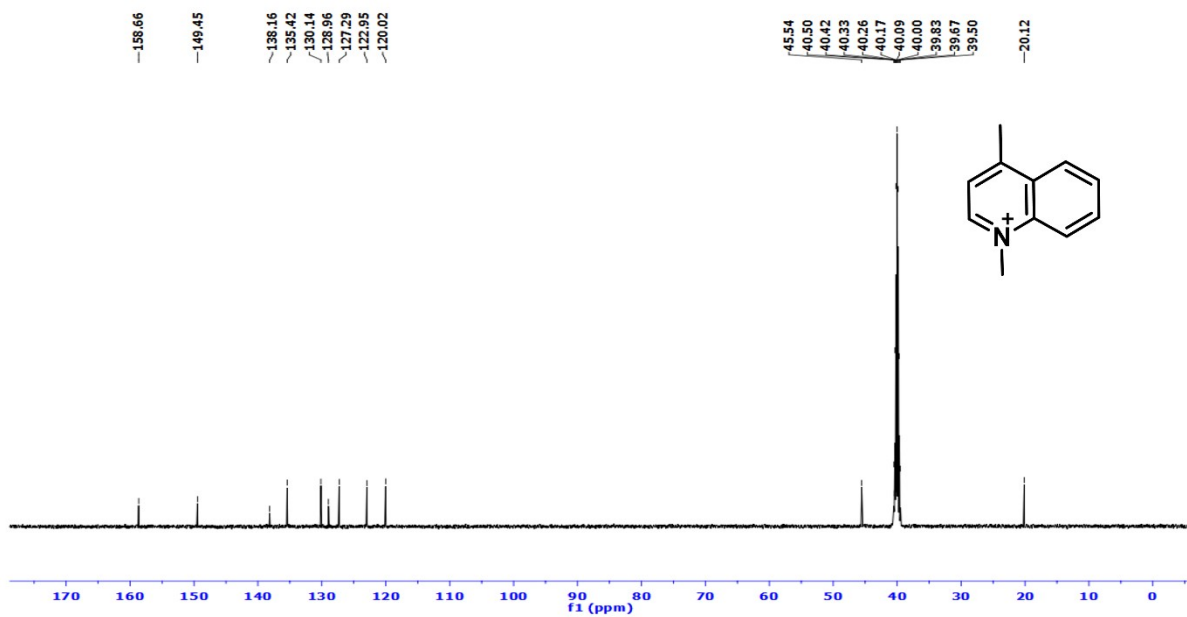


Figure S2. ^{13}C NMR spectrum of 4-QMe

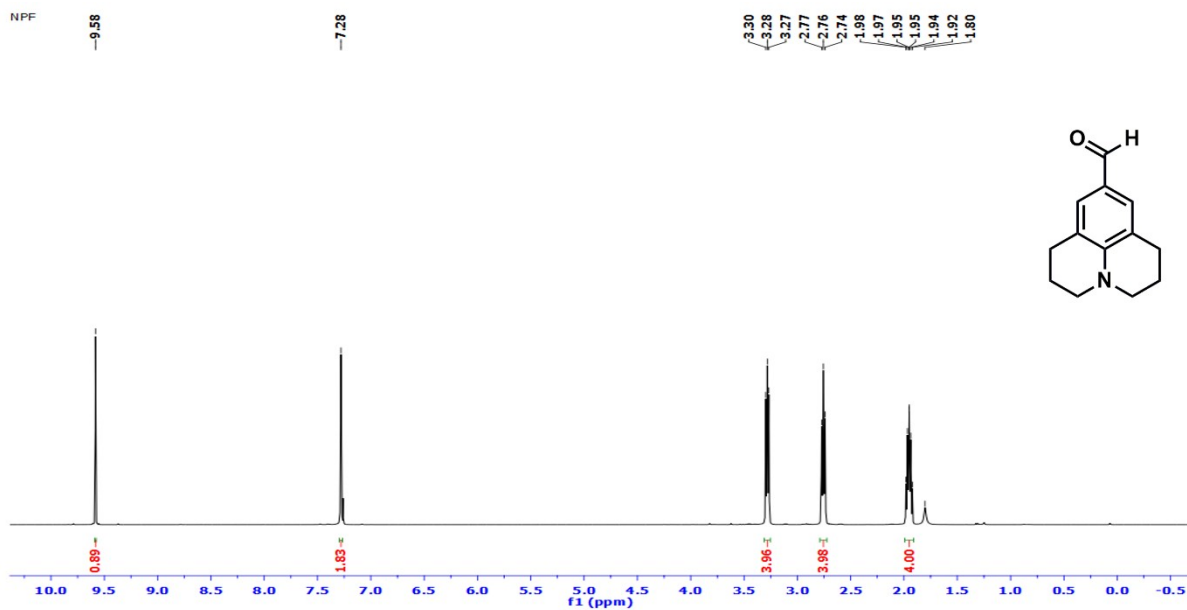


Figure S3. ^1H NMR spectrum of J-CHO

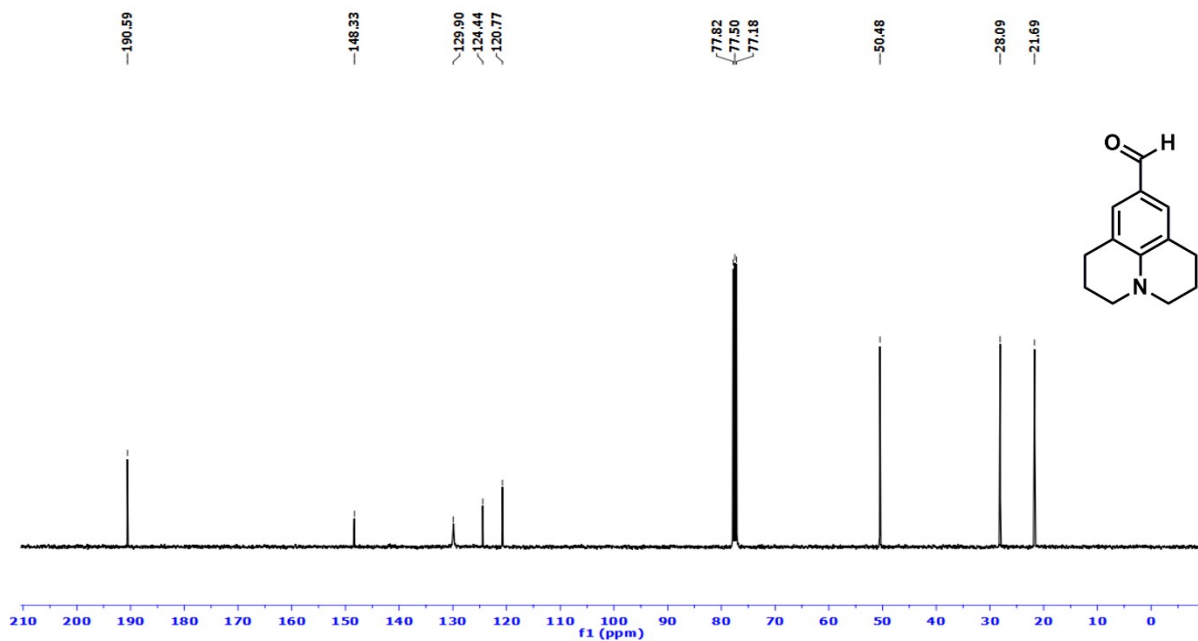


Figure S4. ^{13}C NMR spectrum of J-CHO

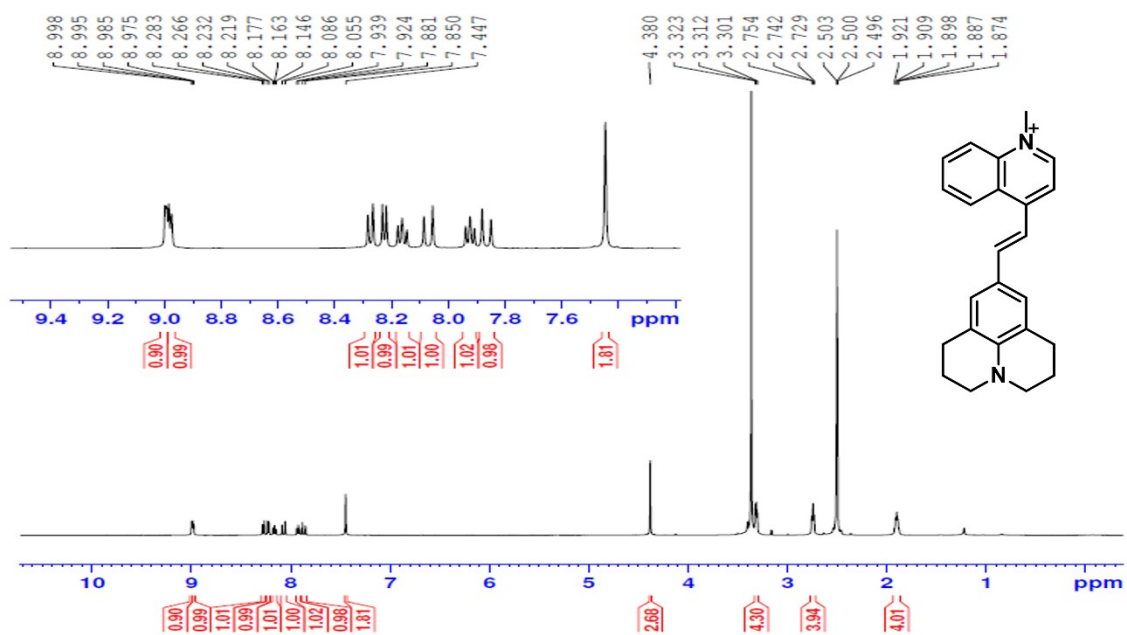


Figure S5. ^1H NMR spectrum of J-QMe

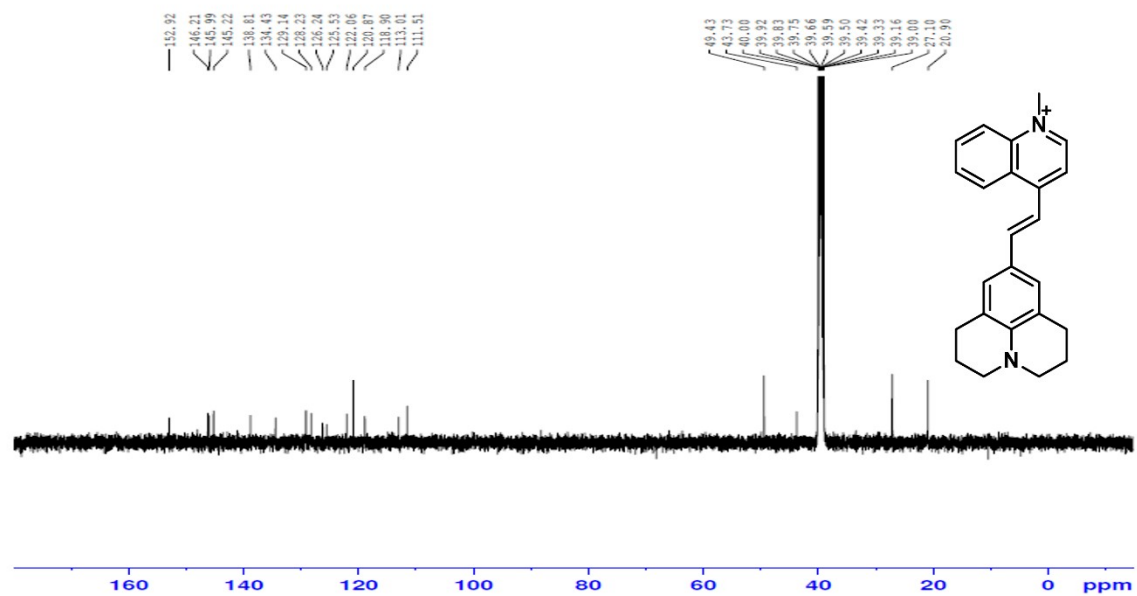


Figure S6. ^{13}C NMR spectrum of J-QMe

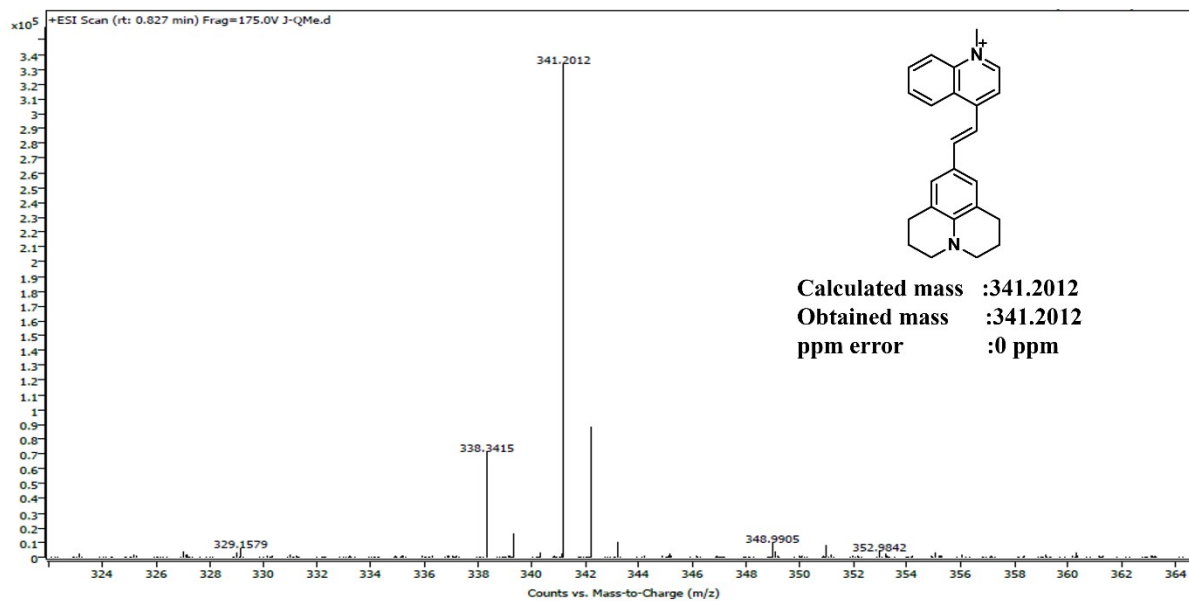


Figure S7. HR-ESI Mass spectrum of J-QMe

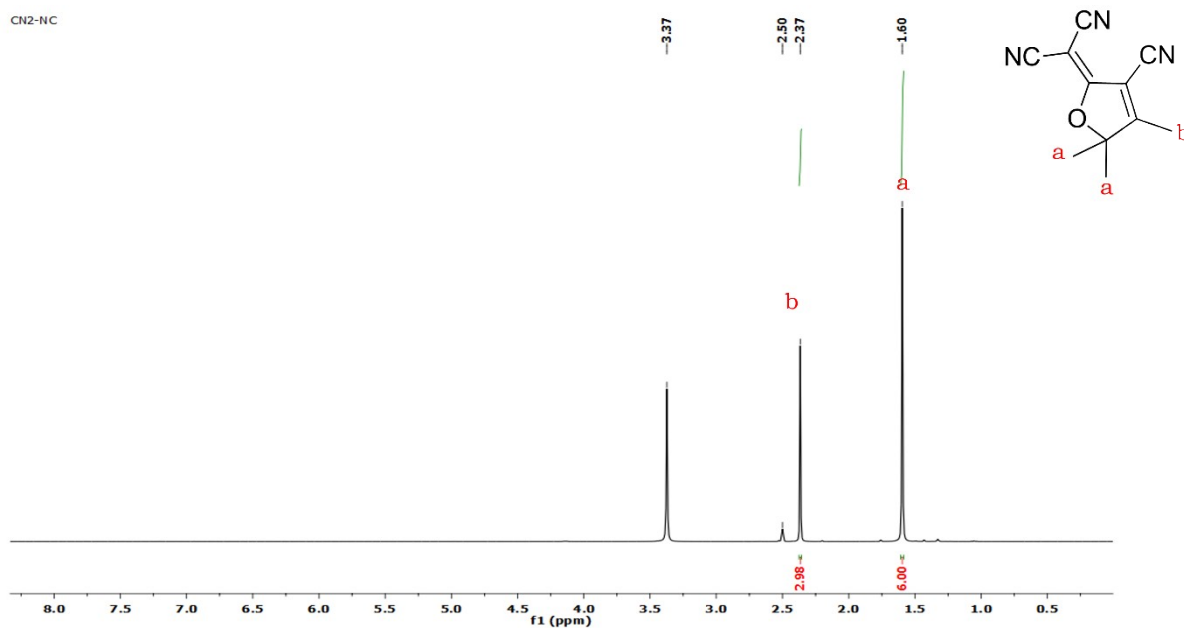


Figure S8. ¹H NMR spectrum of CN-Me

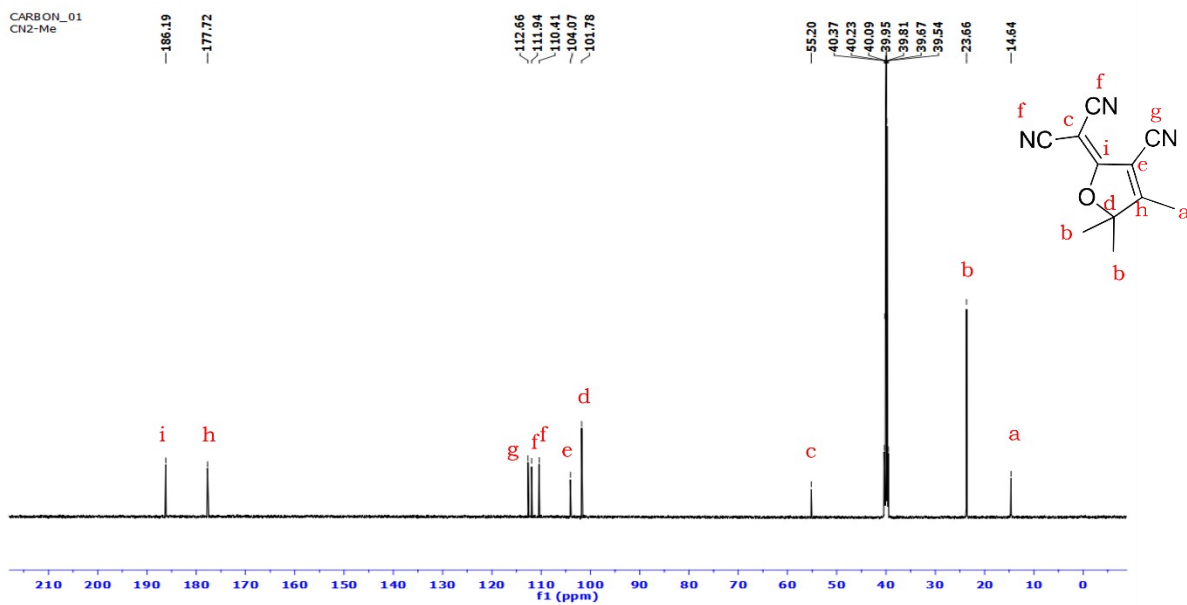


Figure S9. ^{13}C NMR spectrum of CN-Me

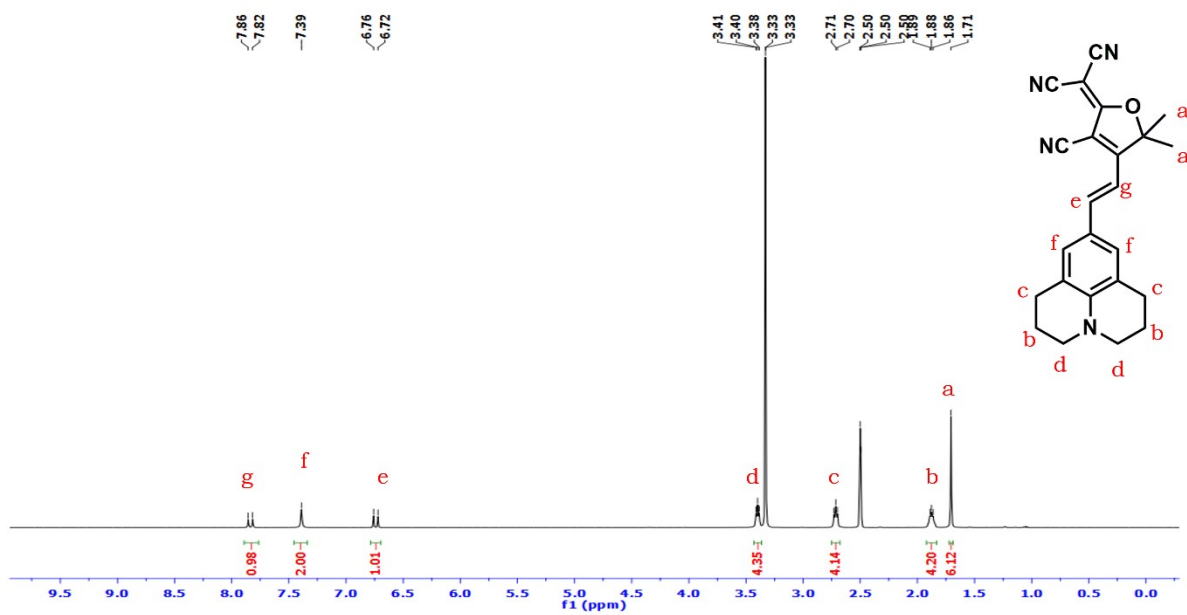


Figure S10. ^1H NMR spectrum of J-CN

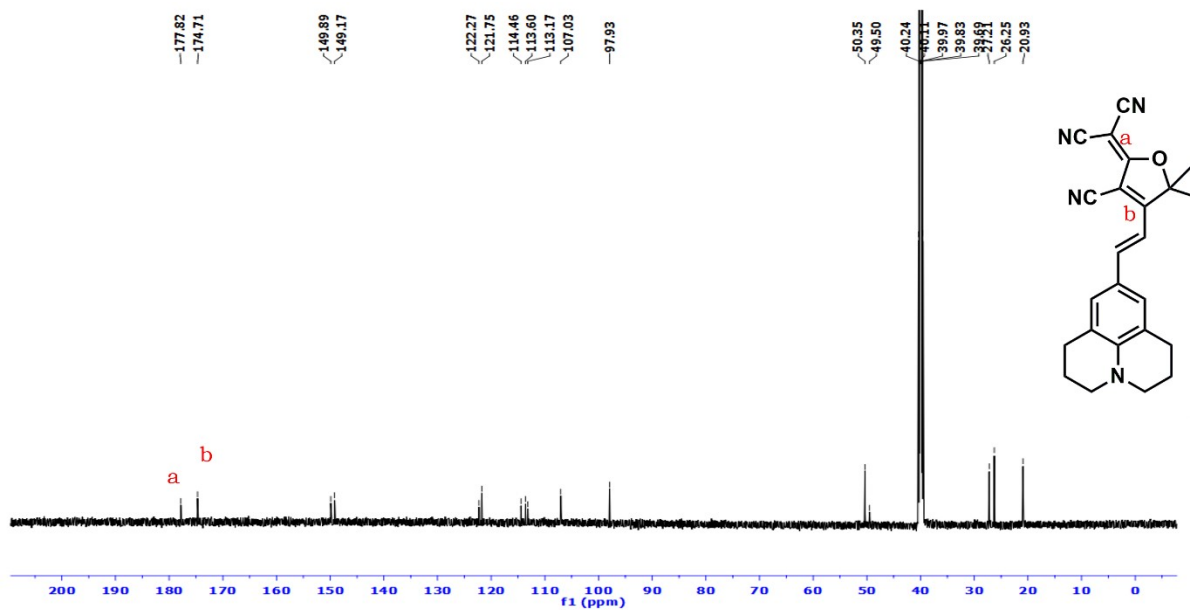


Figure S11. ¹³C NMR spectrum of J-CN

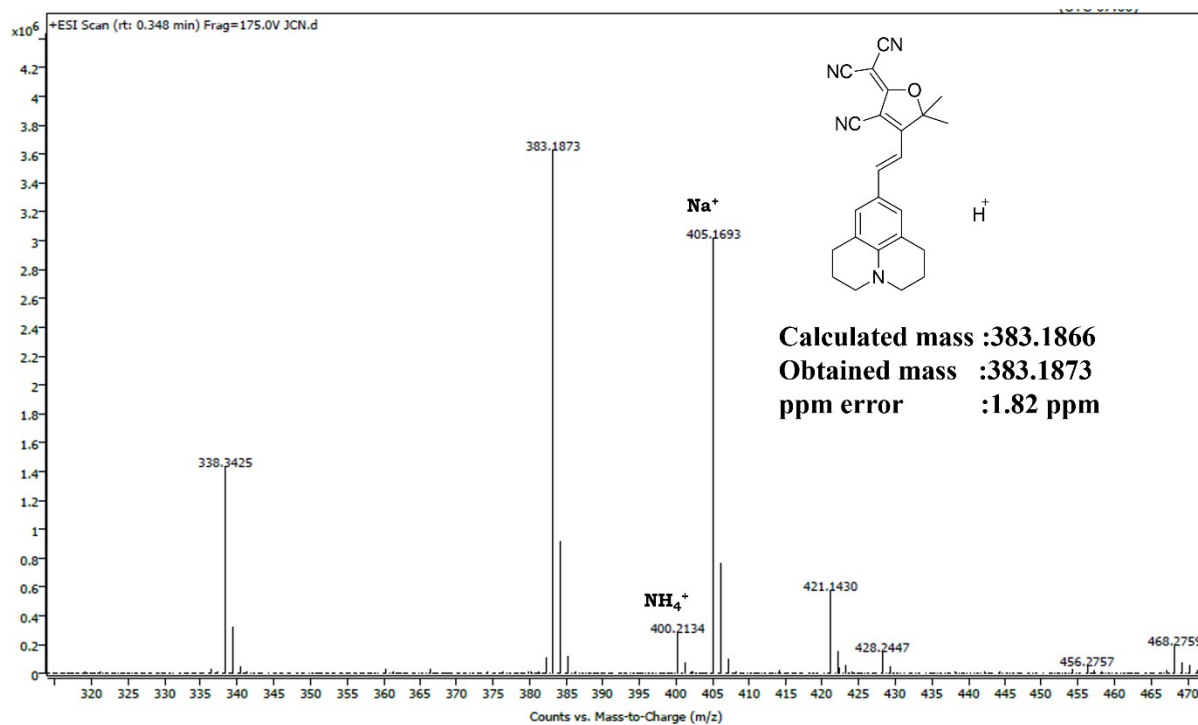


Figure 12. HR-ESI Mass spectrum of J-CN

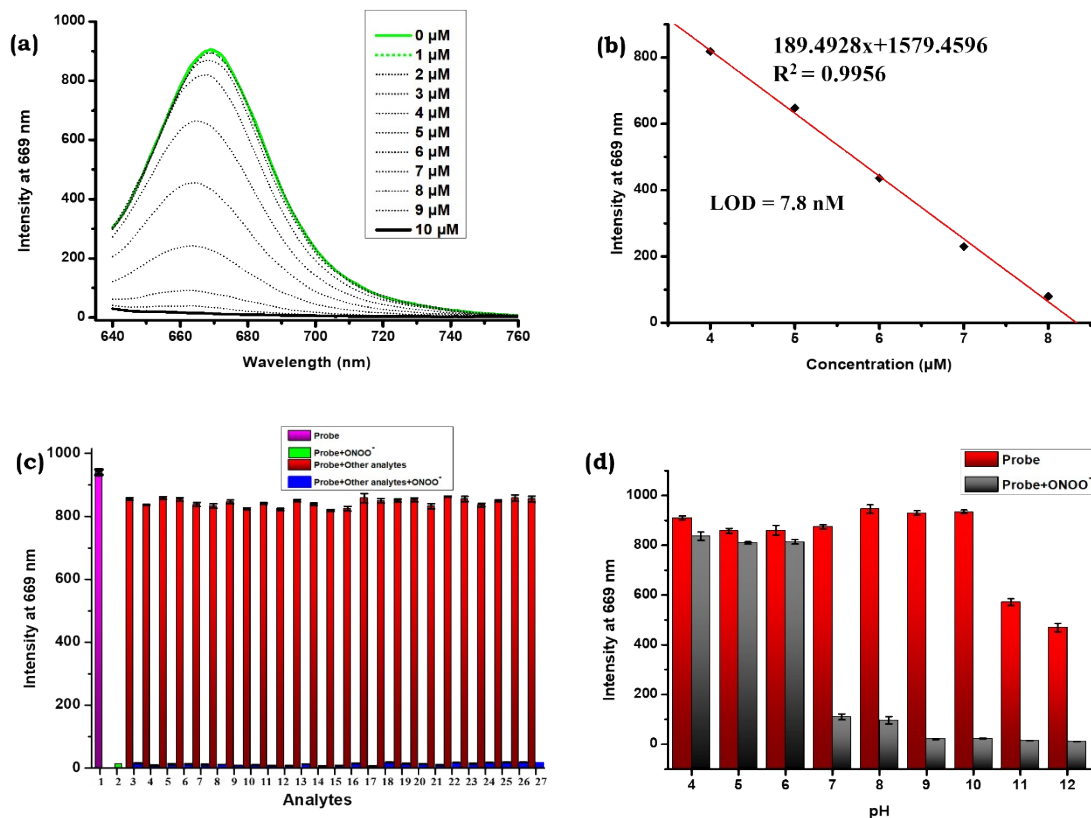


Figure S13 (a) The fluorescence spectra of JCN (5 μM) were recorded upon the addition of ONOO⁻ (10 μM) at various concentrations ranging from 0 to 10 μM. (b) A linear fit was used to plot the JCN emission (5 μM) at 669 nm against the ONOO⁻ concentration (4–8 μM) (c) The intensity at 669 nm was measured for a probe solution (5 μM) that was mixed with ONOO⁻ (10 μM) and other analytes in THF-PBS buffer (1:1) (d) The fluorescence intensity of the probe at 669 nm in THF- PBS (1:1) buffer at varying pH levels when combined with ONOO⁻ (10 μM) [Analytes: (1) Probe, (2) ONOO⁻, (3) Al³⁺, (4) Ca²⁺, (5) Cu²⁺, (6) Fe³⁺, (7) Mg²⁺, (8) Zn²⁺, (9) F⁻, (10) Cl⁻, (11) Br⁻ (12) I⁻, (13) ClO₄⁻, (14) CN⁻, (15) SO₄²⁻, (16) S₂O₃⁻, (17) S₂O₄⁻ (18) HS⁻, (19) H₂O₂, (20) HOCl, (21) TBHP, (22) ¹O₂, (23) O₂⁻, (24) Cys, (25) MesH, (26) Hcy, (27) GSH] [Ex: 620 nm; Em: 640-800nm]

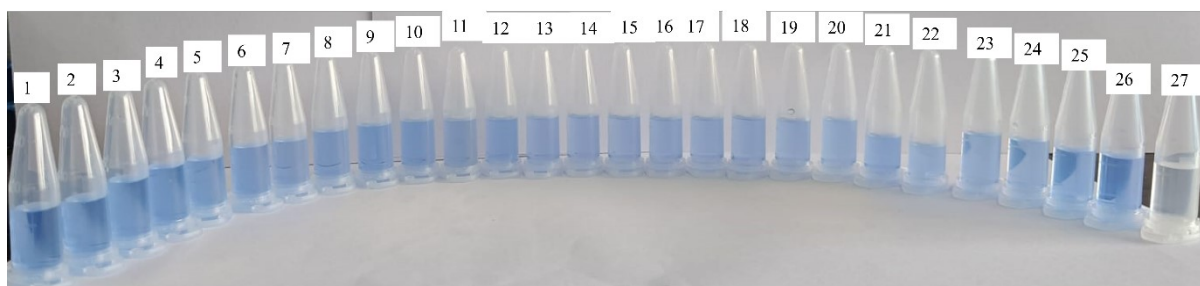


Figure S14. Colour change of the JQMe (20 μM) with different analytes (20 μM) in PBS solution (pH 7.4) under Day light [Analytes: (1) Probe, (2) Al³⁺, (3) Ca²⁺, (4) Cu²⁺, (5) Fe³⁺,

(6) Mg^{2+} , (7) Zn^{2+} , (8) F^- , (9) Cl^- , (10) Br^- , (11) I^- , (12) ClO_4^- , (13) CN^- , (14) SO_4^{2-} , (15) $S_2O_3^{2-}$, (16) $S_2O_4^{2-}$, (17) HS^- , (18) H_2O_2 , (19) $HOCl$, (20) TBHP, (21) 1O_2 , (22) O_2^- , (23) Cys, (24) MesH, (25) Hcy, (26) GSH, (27) $ONOO^-$

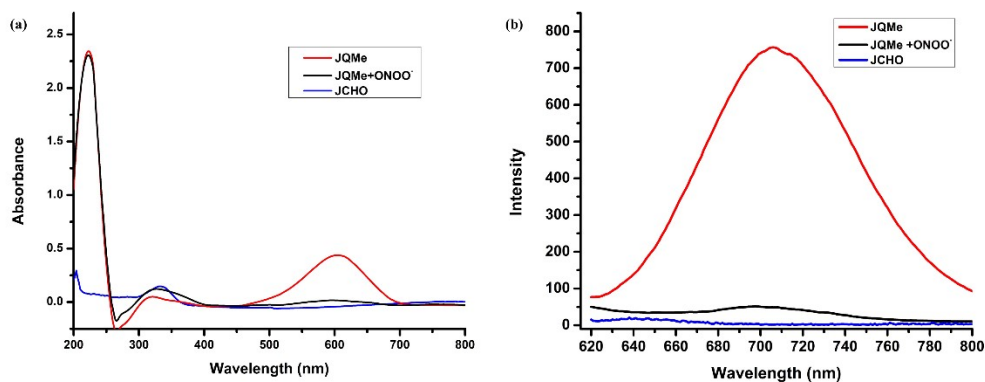


Figure S15. (a) The UV-visible absorption spectrum and (b) fluorescence spectra were measured after adding $ONOO^-$ (20 μM) to a JQMe (20 μM) & JCHO (20 μM) in PBS buffer solution (10 mM, 1:1 v/v) at 37 $^\circ C$

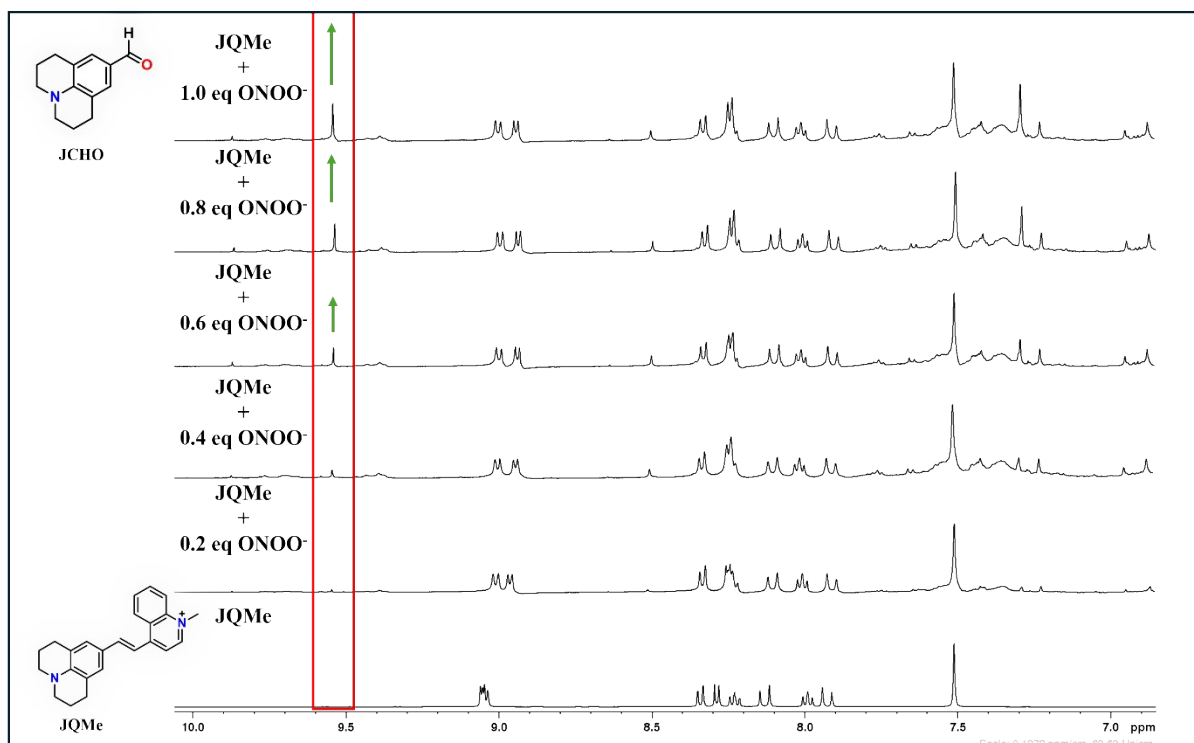


Figure S16. ¹H NMR titration of JQMe with addition of $ONOO^-$ (0-1.0 eq.)

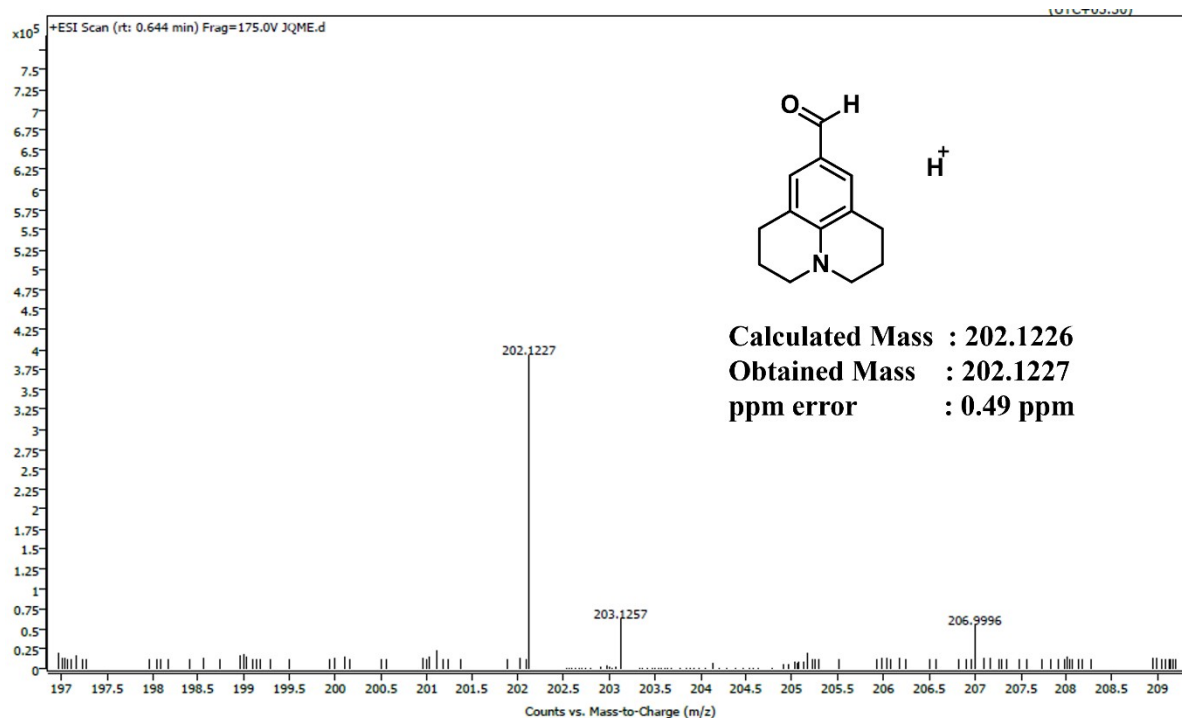


Figure S17. HR-Mass spectrum of JQMe + ONOO⁻

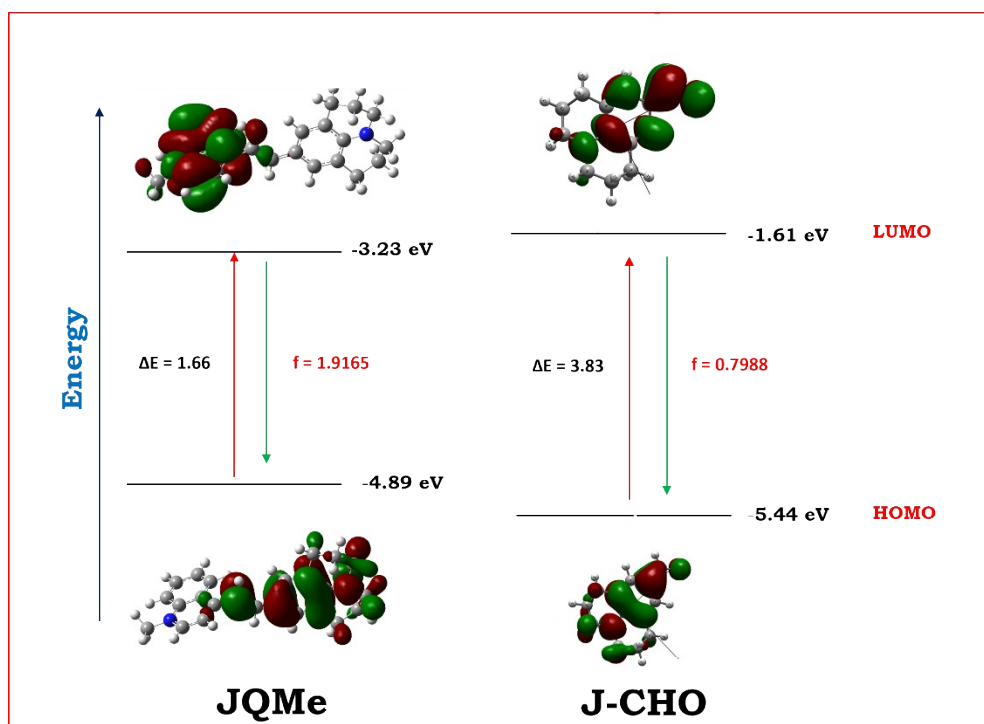


Figure S18. Frontier molecular orbital profiles of JQMe (left) and JCHO (right) based on DFT (B3LYP/631 G*)

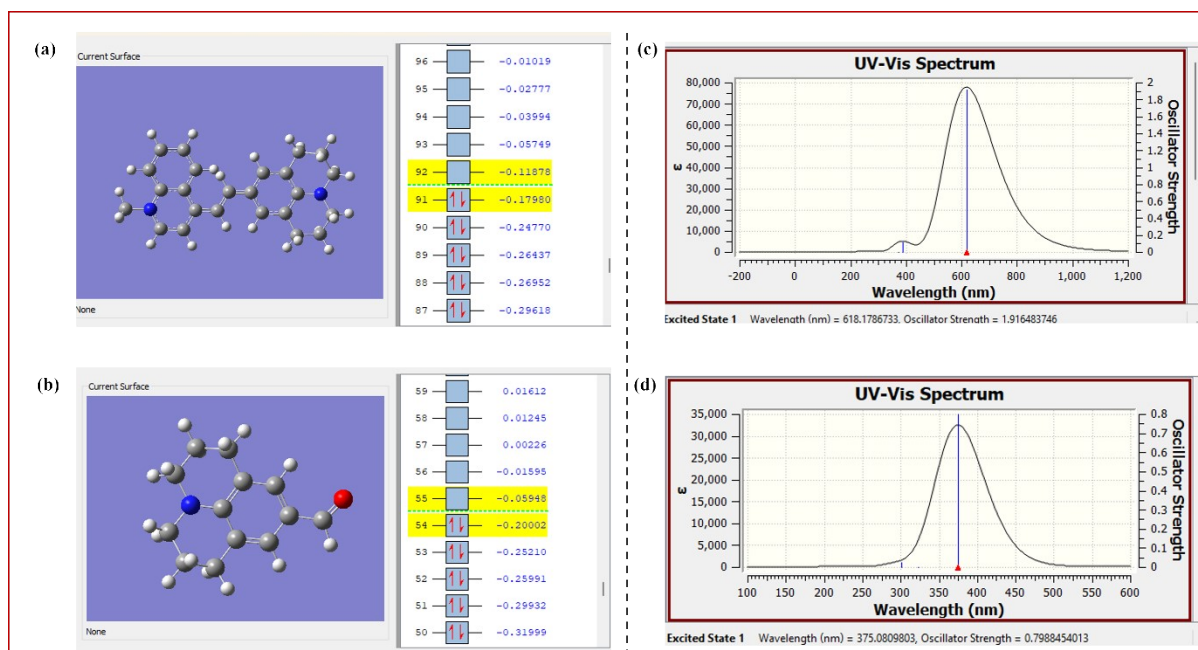


Figure S19. HOMO and LUMO Hartree value of (a) JQMe and (b) JCHO. The oscillator strength values of (c) JQMe and (d) JCHO.

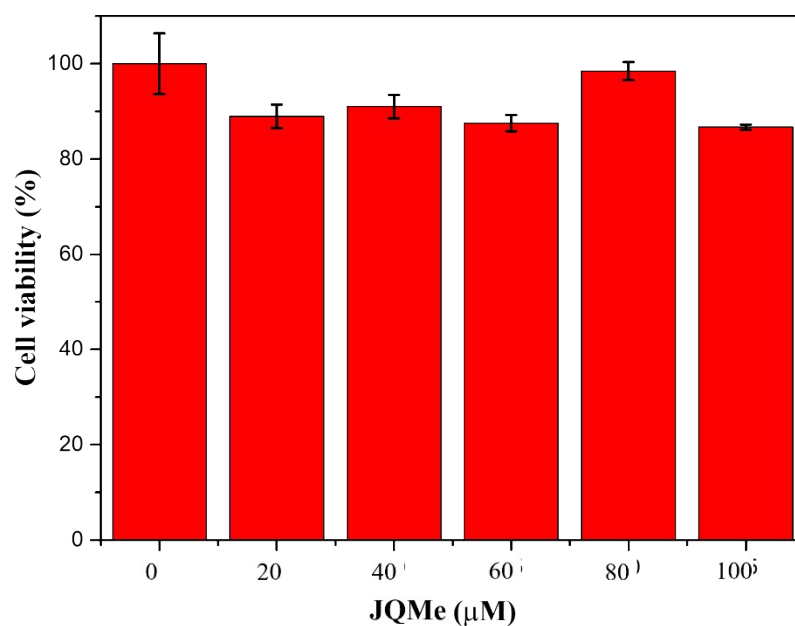


Figure S20. Cell viability of HeLa cells treated with JQMe (0, 20, 40, 60, 80, 100 μM) at 37°C for 24 h. The results are the mean and standard deviation of three independent experiments.

ESI 1. Limit of detection, limit of quantification, and quantum yield calculation

LOD

Detection limit was calculated fluorescence titration data with the equation, based on the definition by IUPAC

$$LOQ = k \times Sb/S$$

Where $k = 3$; S_b is the standard deviation of blank measurement obtained without $ONOO^-$ (Table S2) and 'S' represents slope of the calibration curve (figure 1d).

LOQ

$$LOQ = k \times Sb/S$$

Where $k = 10$; S_b is the standard deviation of blank measurement obtained without $ONOO^-$ (Table S2) and 'S' represents slope of the calibration curve (figure 1d). The limit of quantification was calculated to be $0.02 \mu M$

Table S2. Standard deviation of JQMe ($20 \mu M$) without addition of $ONOO^-$ (I_b is the fluorescence intensity at 706 nm)

	1	2	3	4	5	6	7	8	9	10	S_b
I_b	756.6	756.8	756.7	757.1	756.8	756.7	756.9	756.7	757.1	756.3	0.16

Quantum yield

$$\Phi_S = \Phi_R I_S / I_R * A_R / A_S$$

Φ_S - Quantum yield of sample; Φ_R - Quantum yield of reference (RhB = 0.35)

I_S - Integrated fluorescent area of sample; I_R - Integrated fluorescent area of reference.

A_R - Absorbance of reference; A_S - Absorbance of sample

Table S3. Quantum yield, molar absorptivity and Stokes shift data for JCN and JQMe in different solvents

Solvents	Quantum Yield (Φ)		Molar absorptivity ($L M^{-1} cm^{-1}$)		Stokes shift (nm)	
	JCN	JQMe	JCN	JQMe	JCN ($\lambda_{ex} = 620$ nm)	JQMe ($\lambda_{ex} = 600$ nm)
Methanol	0.035	0.065	9.858×10^4	1.474×10^4	34	108
Ethanol	0.032	0.047	9.636×10^4	1.334×10^4	32	106
Isopropanol	0.030	0.048	10.254×10^4	1.522×10^4	37	118
n-Butanol	0.033	0.060	8.876×10^4	1.635×10^4	68	133
Dimethyl sulfoxide	0.051	0.111	9.260×10^4	1.112×10^4	31	104
Acetonitrile	0.050	0.084	8.576×10^4	0.814×10^4	30	102
Tetrahydrofuran	0.033	0.066	7.314×10^4	0.775×10^4	28	101
Diethyl ether	0.016	0.034	4.040×10^4	0.839×10^4	20	94
Toluene	0.015	0.014	2.382×10^4	0.794×10^4	15	90
Hexane	0.006	0.013	1.982×10^4	0.674×10^4	12	86

Absorbance			Integrated fluorescence area		
Rhodamine-B	JQMe	ONOO ⁻	Rhodamine-B	JQMe	ONOO ⁻
0.6789	0.4416	0.1900	82060.032	18978	5736.676

Table S4. Quantum yield data

Reference

- 1 Q. Li and Z. Yang, *Tetrahedron Lett.*, 2018, **59**, 125–129.
- 2 L. Xia, Y. Tong, L. Li, M. Cui, Y. Gu and P. Wang, *Talanta*, 2019, **204**, 431–437.
- 3 S. Palanisamy, P. Y. Wu, S. C. Wu, Y. J. Chen, S. C. Tzou, C. H. Wang, C. Y. Chen and Y. M. Wang, *Biosens. Bioelectron.*, 2017, **91**, 849–856.
- 4 H. Zhang, J. Liu, Y. Q. Sun, Y. Huo, Y. Li, W. Liu, X. Wu, N. Zhu, Y. Shi and W. Guo, *Chem. Commun.*, 2015, **51**, 2721–2724.
- 5 S. V. Mulay, Y. Kim, K. J. Lee, T. Yudhistira, H. S. Park and D. G. Churchill, *New J. Chem.*, 2017, **41**, 11934–11940.
- 6 B. Guo, J. Jing, L. Nie, F. Xin, C. Gao, W. Yang and X. Zhang, *J. Mater. Chem. B*, 2018, **6**, 580–585.
- 7 J. Li, J. Tang, X. Yang, P. Xie, J. Liu, D. Zhang and Y. Ye, *Sensors Actuators B Chem.*, 2022, **358**, 131513.
- 8 M. Yan, H. Fang, X. Wang, J. Xu, C. Zhang, L. Xu and L. Li, *Sensors Actuators, B Chem.*, 2021, **328**, 1–7.
- 9 X. Xie, Y. Liu, G. Liu, Y. Zhao, J. Bian, Y. Li, J. Zhang, X. Wang and B. Tang, *Anal. Chem.*, 2022, **94**, 10213–10220.
- 10 S. Chen, W. Huang, H. Tan, G. Yin, S. Chen, K. Zhao, Y. Huang, Y. Zhang, H. Li and C. Wu, *Analyst*, 2023, **148**, 4331–4338.